Ligand- and solvent-free ATRP of MMA with FeBr 3 and inorganic salts

Jirong Wang, Xiaolin Xie, Zhigang Xue, Christophe Fliedel, Rinaldo Poli

ARTICLE

Ligand- and solvent-free ATRP of MMA with $FeBr_3$ and inorganic salts

Received 00th January 20xx,
Accepted 00th January 20xx

DOI: 10.1039/x0xx00000x

Jirong Wang,[a] Xiaolin Xie,[a] Zhigang Xue,*[a] Christophe Fliedel,[b] and Rinaldo Poli*[b,c]

The bulk methyl methacrylate (MMA) polymerisation can be achieved with excellent control by ATRP in the presence of $FeBr_3$/EBrPA/Mt^+X^-, where EBrPA = ethtyl 2-bromophenylacetate and Mt^+X^- can be one of several inorganic compounds (carbonate, bicarbonate, phosphate, hydroxide, chloride, bromide) of an alkali metal cation. The most effective cations are sodium and potassium. Notably, this procedure does not require the presence of any neutral ligand or coordinating solvent. The polymer chain end analysis demonstrates the initiator action of EBrPA. A mechanistic investigation shows that the ATRP activator, $FeBr_2$, is generated *in situ* after EBrPA activation by the inorganic salt, deactivation of the resulting EPA radical by $FeBr_3$, and quenching of the concurrently generated $Mt^+(XBr^\bullet)^-$ radical. This quenching occurs by addition to MMA, but it is also possible by Fe-catalysed disproportionation when MtX = KOH. The EPA radical may also terminate by dimerisation and the removal of these reducing equivalents is detrimental to the $FeBr_2$ accumulation, but the removal of the oxidizing $Mt^+(XBr^\bullet)^-$ equivalents prevails. The mechanistic investigation also confirms that the product of Br addition to MMA, methyl 1,2-dibromoisobutyrate, is not an efficient initiator for the MMA ATRP catalysed by $FeBr_2$ under thermal conditions.

Introduction

Atom transfer radical polymerisation (ATRP) has been intensively investigated thanks to its intriguing capability of producing well-defined polymers with predictable molecular weights as well as narrow molecular weight distributions.[1-4] A key issue, in the typical implementation of ATRP, is the selection of appropriate organic ligands, with which the catalyst solubility and the activation rate constant can be dramatically altered.[5] Various kinds of transition metals have been employed, particularly copper. Iron, however, is a metal of great interest, owing to its considerable versatility, low toxicity, relatively lower cost and adaptability to a wide variety of monomers.[6, 7] ATRP can be initiated by either direct or inverse strategies, both leading to the same moderating equilibrium. For a Fe^{II}/Fe^{III} ATRP system, the direct strategy requires the simultaneous presence of a halogen-containing initiator R_0-Y and an activating L/Fe^{II} complex capable of abstracting the halogen atom to yield L/Fe^{III}-Y and $R_0^\bullet$. In the reverse strategy, a conventional source of $R_0^\bullet$ (I) can be used in the presence of a deactivating L/Fe^{III}-Y complex (Scheme 1).

Quite a bit of attention was given to the reverse initiation method, since Fe^{III} systems are air-stable and easier to handle than the Fe^{II} analogues. For what concerns the polymerisation of MMA, the controlling equilibrium was achieved under typical reverse ATRP conditions from systems such as L/FeX_3 (X = Cl, Br; L = neutral ligand) or $Fe(dtc)_3$ (dtc = *N,N*-diethyldithiocarbamate, Et_2NCS_2) and a variety of radical thermal initiators such as AIBN,[8] 1,1,2,2-tetraphenyl-1,2-ethanediol,[9] diethyl 2,3-dicyano-2,3-diphenylsuccinate,[10] tetraethylthiuram disulfide[11-13] or photoinitiators such as 2,2-dimethoxy-2-phenylacetophenone.[14] Fe^{III} systems were also used to generate the Fe^{II} activator complexes *in situ* in the presence of reducing agents (AGET or ARGET strategies)[15, 16] or in the presence of conventional radical initiators (ICAR strategy).[17-19]

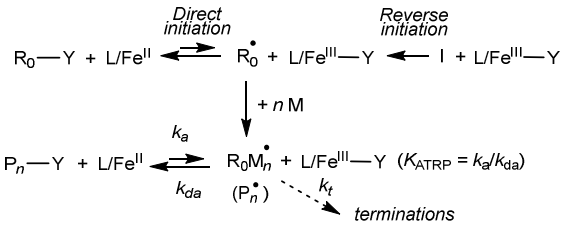

Scheme 1. Direct and reverse initiating methods for an L/Fe^{II}-catalysed ATRP.

In 2000, Qiu and coworkers showed that a Fe^{III} system, notably $Fe(dtc)_3/FeCl_3/PPh_3$, may be used in the absence of any organic halide, radical sources or reducing agents to initiate the MMA polymerisation.[20] This system spontaneously produces Fe^{II} and Et_2NCS_2Cl, yielding polymers with α-Et_2NCS_2 and ω-Cl chain ends. In 2008, Noh and coworkers showed that the $FeBr_3$/L/EBiB system (L = phosphine ligand, EBiB = ethyl bromoisobutyrate) is able to initiate the MMA polymerisation and proposed that the monomer itself is able to reduce the Fe^{III} complex to produce the activator ($FeBr_2$/L) *in situ*,[21-24] although it was later proposed

[a] Key Laboratory for Material Chemistry of Energy Conversion and Storage, Ministry of Education, School of Chemistry and Chemical Engineering, Huazhong University of Science and Technology, Wuhan 430074, P. R. China.
[b] CNRS, LCC (Laboratoire de Chimie de Coordination), Université de Toulouse, UPS, INPT, 205 Route de Narbonne, BP 44099, F-31077 Toulouse Cedex 4, France.
Institut Universitaire de France, 1, rue Descartes, 75231 Paris Cedex 05, France
Electronic Supplementary Information (ESI) available: experimental details, tables of raw polymerisation data, graphs of MMA polymerisations, polymer characterisation (20 pages). See DOI: 10.1039/x0xx00000x.

that the metal complex may in fact be reduced by the phosphine ligand.[25, 26] Hence, a claim that a Fe^{III} complex with a phosphine ligand is able to play an activator role does not appear credible.[27] However, a more recent report by the Noh group has shown that the FeX_3/L system (X = Cl, Br; L = phosphine ligand) also works without external initiator, producing PMMA-X chains and provided some evidence that these chains contain a $-C(CH_3)(COOCH_3)(CH_2X)$ α-chain end.[28] Thus, MMA would indeed appear to be able to reduce the Fe^{III} salt, potentially generating methyl 1,2-dihaloisobutyrate, $CH_3C(X)(CH_2X)COOCH_3$. In this molecule, the CH_2-X bond is inactive and only the bond on the tertiary C atom would be activated to enter into the standard ATRP moderating equilibrium. However, it was subsequently shown that methyl 1,2-dibromoisobutyrate is unable to initiate the MMA radical polymerisation in the presence of $FeBr_2$ and PPh_3 under thermal conditions.[29] In addition, it was shown in another recent contribution that $FeBr_3$/MeCN is reduced to $FeBr_2$/MeCN by stoichiometric amounts of MMA (Fe:MMA = 2:1), to yield methyl 1,2-dibromobutyrate, but only under the action of UV irradiation.[30] In the presence of a large MMA excess and ethyl 2-bromophenylpropionate (EBrPA) as initiator, a well-controlled photopolymerisation occurred at room temperature, but the polymerisation stopped in the absence of light. In an additional contribution, the same group reported that this system, like the Noh system, also works in the absence of external initiator, yielding PMMA that supposedly contains CH_3C-CH_2Br-$C(COOCH_3)$-chain ends.[31]

We have recently reported that many inorganic salts such as halides, carbonates, sulfates, hydroxide, etc., in the absence of ATRP catalysts, activate EBrPA and promote the radical polymerisation of MMA.[32] These polymerisations proceed without controlled chain growth, except for the iodide salts. However, in combination with $FeBr_2$, excellent control was observed for all those salts, particularly in the presence of a small amount (10%) of $FeBr_3$.[33] These polymerisations are regular ATRP systems with direct activation by the combination of a halide initiator (EBrPA) and an activator, which is generated *in situ* from $FeBr_2$ and the salt additive. In the present contribution, we show that an excellent control, in fact an even better one, is obtained when the above system is modified by replacing $FeBr_2$ with $FeBr_3$. The genesis of the activator, namely the reduction mechanism of $FeBr_3$ to $FeBr_2$ and the identity of the associated products are addressed in detail. The conditions described in this contribution constitute a new way to produce PMMA materials rapidly and with excellent control under simple operating conditions (bulk, low temperatures) starting from non-toxic, inexpensive and bench stable compounds ($FeBr_3$, inorganic salts). They still require, however, using an efficient halide initiator (EBrPA).

Results and Discussion

(a) Polymerisations with $FeBr_3$ and alkali metal carbonates.

The MMA polymerisation, carried out in bulk at 60°C, with $FeBr_3$ as catalyst, Na_2CO_3 as additive and EBrPA as initiator ([MMA]:[$FeBr_3$]:[Na_2CO_3]:[EBrPA] = 800:1:8:4) led to a 62.1% monomer conversion in 11.5 h and yielded a PMMA with M_n very close to expected value and low dispersity (1.1), see Table 1, entry 1. Control experiments indicate that all components of this system are necessary to provide a relatively rapid and well-controlled polymerisation: no polymer was obtained using $FeBr_3$ either alone (entry 2) or in the presence of EBrPA (entry 3) without Na_2CO_3, and only 8.3% in 24 h when using $FeBr_3$ and Na_2CO_3 without initiator and the recovered polymer had a very high molar mass (entry 4). Clearly, the combined action of the monomer, the EBrPA initiator, and the Na_2CO_3 additive at the polymerisation temperature must result in partial transformation of the $FeBr_3$ deactivator into the $FeBr_2$ activator. The polymerisation of entry 1 is slower than that carried out under similar conditions with $FeBr_2$ instead of $FeBr_3$ (after 300 min, 75.5 % conversion was obtained in the absence of $FeBr_3$ and 64.3% in the presence of 10% $FeBr_3$).[33] This obviously results from a lower activator/deactivator ratio in the present case, because the observed polymerisation rate depends linearly on $[Fe^{II}]/[Fe^{III}]$. For the previously reported polymerisation with $FeBr_2$,[33] a little amount of $FeBr_3$ accumulates during the initial phase of the polymerisation because of the irreversible chain terminations. Conversely, the use of $FeBr_3$ generates a little amount of $FeBr_2$ during the initial phase (the mechanism of this transformation is thoroughly discussed in a later section). Using $FeBr_3$ gives, however, a product with a narrower molar mass distribution. The result of entry 4 is particularly noteworthy in light of the previous report of relatively rapid and well-controlled polymerisations with $FeBr_3$/phosphine ligand in the absence of external initiator (e.g. conversions up to 60% in 15 min at 80°C, Đ < 1.2).[28] This suggests that the $FeBr_3$/phosphine ligand system is more efficient than the $FeBr_3$/Na_2CO_3 system. Table 1 also shows the results of the previously published MMA polymerisation in the presence of initiator and Na_2CO_3 but without any Fe catalyst (entry 5), which gave a lower yield, even at a much higher temperature, and an uncontrolled polymerisation.[32]

The polymerisation of entry 1 follows first-order kinetics (Figure 1a) in line with a constant radical concentration and is characterised by an induction time, which is related to the need to reduce part of the $FeBr_3$ catalyst to the $FeBr_2$ activator. The good control is demonstrated by the excellent match between observed and calculated molar masses and by the low Đ values (Figure 1b). Similar results were obtained in the presence of potassium carbonate (Figure 1), with a barely lower observed rate constant and a smaller induction time. The raw data related to these polymerisations are available in the Supporting Information (Table S1). The isolated purified polymer was chain extended in a separated experiment using a [MMA]:[$FeBr_3$]:[Na_2CO_3]:[PMMA-Br] ratio of 500:0.25:2:1 at 60°C. The GPC monitoring showed a regular progression of the molar masses while the dispersity remained low and no low-molar mass tailing of the distribution could be noticed in the GPC traces (see Table S2 and Figure S1), indicating an excellent chain-end fidelity for the PMMA-Br macroinitiator.

ARTICLE

Table 1. EBrPA-initiated MMA bulk polymerisation in the presence of $FeBr_3/Na_2CO_3$ and control experiments.[a]

Entry	Na_2CO_3/MMA	EBrPA/MMA	$FeBr_3$/MMA	T/°C	t/h	Conv. /%	$M_{n,GPC}(M_{n,th})$/Kg mol^{-1}, Đ	Ref.
1	0.01	0.005	0.00125	60	11.5	62.1	11.3(12.4), 1.1	This work
2	0	0	0.00125	60	24	0	-	This work
3	0	0.005	0.00125	60	24	0	-	This work
4	0.01	0	0.00125	60	24	8.3	1449.3(1.7)[b], 1.33	This work
5	0.01	0.005	0	90	12	21.9	483.2(4.4), 2.46	[32]

[a]Conditions: [MMA]:[$FeBr_3$]:[Na_2CO_3]:[EBrPA] = 200:0.25:2:1; T = 60°C. [b] $M_{n,th}$ based on the production of methyl 2,3-dibromoisobutyrate.[30]

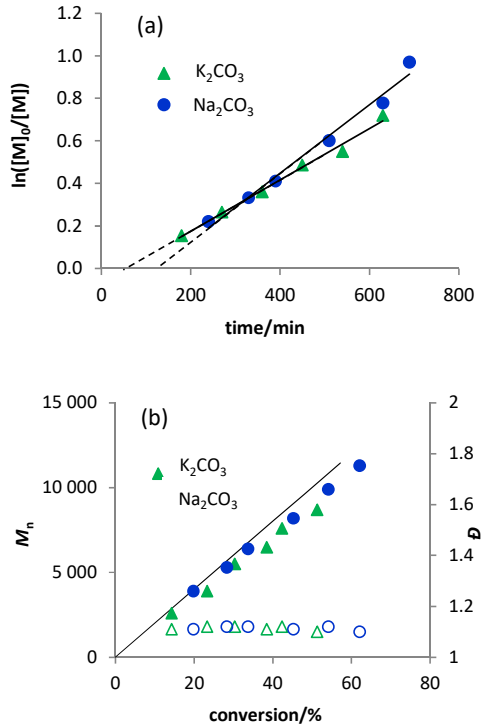

Figure 1. First-order plots (a) and evolution of M_n and $Đ$ with conversion (b) for the bulk $FeBr_3$-catalysed and EBrPA-initiated MMA polymerisation in the presence of alkali metal carbonate. [MMA]:[$FeBr_3$]:[Cat_2CO_3]:[EBrPA] = 200:0.25:2:1 (Cat = Na, K), T = 60°C.

Since the recent contribution by Matyjaszewski and co-workers has shown that light has an effect on the MMA polymerisation rate under conditions similar to ours ($FeBr_3$ without reducing agents or radical sources, although at room temperature and in MeCN solution)[30] the polymerisation with $FeBr_3/Na_2CO_3$ was repeated in the dark. The results are quite similar to those obtained with the laboratory light (Figure S2), demonstrating the thermal nature of the activator generation process.

The Na_2CO_3 system was investigated in greater details. Using different MMA/EBrPA ratios in the 200-1000 range, while keeping the same [$FeBr_3$]:[Na_2CO_3]:[EBrPA] proportions (0.25:2:1), gave equally well-controlled polymerisations with molar masses close to target and low dispersities, while the k_{obs} scaled inversely with the MMA/EBrPA ratio (see SI, Table S3 and Figure S3). In addition to EBrPA, several other initiators were tested for this polymerisation, always keeping the same [MMA]:[$FeBr_3$]:[Na_2CO_3]:[EBrPA] molar ratio and polymerisation temperature. The results (SI, Table S4 and Figure S4) show that methyl and ethyl 2-bromoisobutyrate (MBiB, EBiB) and 2-bromopropionitrile (BPN) also lead to well-controlled polymerisations, whereas (1-bromoethyl)benzene (PEBr), methyl and ethyl 2-bromopropionate (MBrP, EBrP) gave lower initiation efficiencies, as evidenced by the discrepancy between the observed and theoretical molar masses, although acceptable dispersities were always obtained. Polymerisations with the EBrPA initiator and under identical conditions to those in Figure 1 ([MMA]:[$FeBr_3$]:[Na_2CO_3]:[EBrPA] = 200:0.25:2:1) were run in the 60-90°C temperature range. The results, see Figure 2 (raw data in Table S5) indicate that the polymerisation remains well-controlled under all conditions, with only barely higher Đ at the highest conversion at 90°C (1.17).

While keeping all other parameters constant, the polymerisation was repeated at different $Na_2CO_3/FeBr_3$ ratios, yielding the results shown in Figure 3 (data in Table S6). While the polymerisation remained equally well-controlled for all ratios, the observed rate constant decreased when the amount of Na_2CO_3 was lowered to 0.5 equivalents and remained essentially unchanged when it was increased to 3 equivalents. The same study for the $FeBr_2$/KBr system showed a similar effect, with k_{obs} reaching a plateau beyond the equimolar KBr/$FeBr_2$ ratio.[33] As discussed in detail in that contribution with the support of DFT calculations, this effect could be attributed to the addition of the bromide ion from KBr to generate $K[FeBr_3]^-$, which is a more active form of the catalyst.[33] Therefore, Na_2CO_3 also appears to generate an adduct, $Na_{2n}[FeBr_2(CO_3)_n]^{2n-}$, having greater activity. An excess amount of the sparingly soluble Na_2CO_3 is not expected to further increase the activity because the reaction medium is saturated. This effect is not the same as that of certain other additives, such as phosphines,[27] where a greater amount of additive increases the extent of $FeBr_3$ reduction. In the present case, the

carbonate salt cannot act as reducing agent and may only affect the speciation of the already generated Fe^{II} activating system.

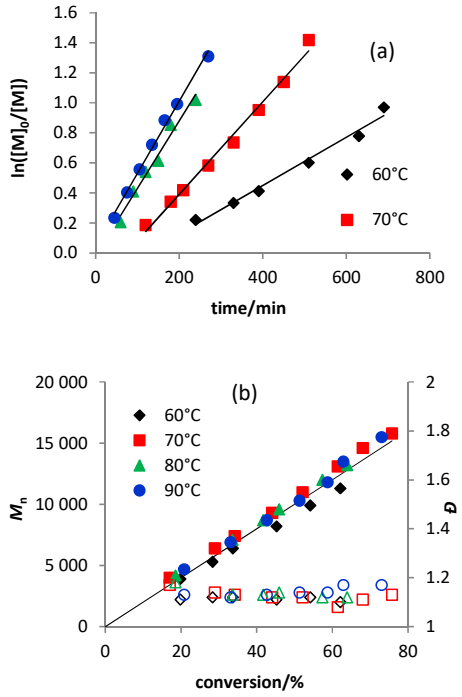

Figure 2. First-order plots (a) and evolution of M_n and $Đ$ with conversion (b) for the EBrPA-initiated bulk MMA polymerisation catalysed by the $FeBr_3/Na_2CO_3$ system at different temperatures. [MMA]:[$FeBr_3$]:[Na_2CO_3]:[EBrPA] = 200:0.25:2:1.

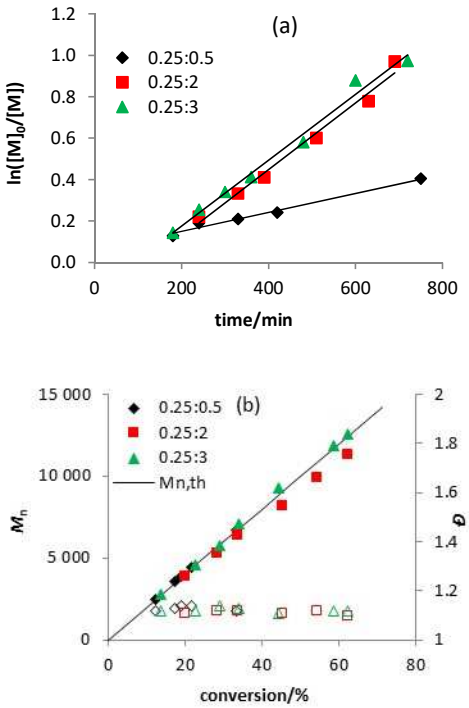

Figure 3. First-order plots (a) and evolution of M_n and $Đ$ with conversion (b) for the EBrPA-initiated bulk MMA polymerisation catalysed by the $FeBr_3/Na_2CO_3$ system at different [$FeBr_3$]:[Na_2CO_3] ratios. [MMA]:[$FeBr_3$]:[Na_2CO_3]:[EBrPA] = 200:0.25:x:1; T = 60°C.

Polymerisations were also carried out with increasing $FeBr_3$ amounts relative to the EBrPA initiator. Once again, all polymerisations were well-controlled (Figure 4, data in Table S7). In this case, approximately equivalent k_{obs} values were observed for the lower $FeBr_3$ amount experiments, whereas using an equimolar amount relative to EBrPA significantly reduced the polymerisation rate. This effect is probably caused by a decrease of the activator/deactivator ratio. The fraction of Fe^{II} activator that is self-generated under polymerisation conditions probably no longer increases proportionally with the amount of added deactivator.

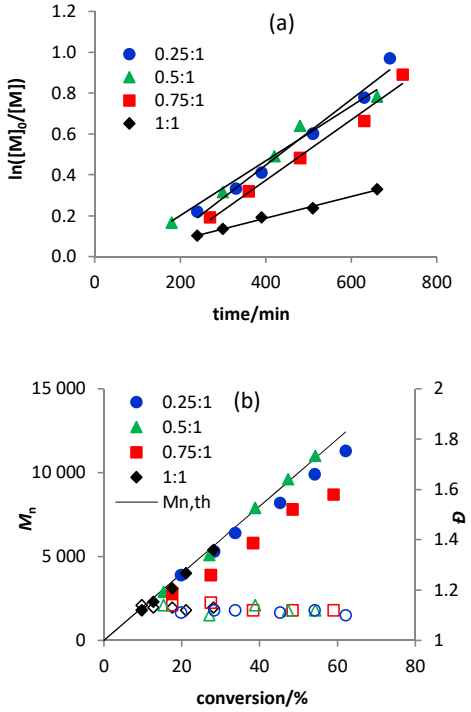

Figure 4. First-order plots (a) and evolution of M_n and $Đ$ with conversion (b) for the EBrPA-initiated bulk MMA polymerisation catalysed by the $FeBr_3/Na_2CO_3$ system at different [$FeBr_3$]:[EBrPA] ratios. [MMA]:[$FeBr_3$]:[Na_2CO_3]:[EBrPA] = 200:x:2:1; T = 60°C.

(b) Polymerisations with $FeBr_3$ and other basic salts.

In addition to the sodium and potassium carbonates, polymerisations were also run with the corresponding bicarbonates, hydroxides, and potassium phosphate. The main features of these polymerisations are quite similar to those with the $FeBr_3/Na_2CO_3$ system shown above. All raw data are collected in Table S8. The bicarbonates and phosphate systems (Figure S5) behaved similarly to the carbonates under the same standard conditions (60°C, [MMA]:[$FeBr_3$]:[salt]:[EBrPA] = 200:0.25:2:1), with K_3PO_4 yielding a polymerisation rate (k_{obs} = $1.8 \cdot 10^{-3}$ min^{-1}) quite close to that of Na_2CO_3 (k_{obs} = $1.6 \cdot 10^{-3}$ min^{-1}), whereas the rates in the presence of $NaHCO_3$ ($8.5 \cdot 10^{-4}$ min^{-1}) and $KHCO_3$ ($7.8 \cdot 10^{-4}$ min^{-1}) are smaller than that of and K_2CO_3 ($1.2 \cdot 10^{-3}$ min^{-1}). The two hydroxide systems, on the other hand, were well-behaved only when using a larger amount of $FeBr_3$ (1 equivalent relative to EBrPA), see Table S8 and Figure S6.

(c) Polymerisations with $FeBr_3$ and chloride or bromide salts.

In the presence of a chloride or bromide salt, $FeBr_3$ also leads to the controlled polymerisation of MMA with molar masses in agreement with the target values and reasonably low dispersities, but the polymerisations are slower than with the basic salts described above, requiring operations at 90°C in order to obtain reasonable rates. For the bromide series, as shown in Table 2 (entries 1-5), the rate strongly depends on the nature of the cation. The highest rates are obtained in the presence of NaBr and KBr, whereas LiBr leads to a very slow but still controlled polymerisation and the Rb and Cs salts give no polymer at all. The same cation effect was previously observed and rationalized in the investigation of the EBrPA activation by MtBr (Mt = Li, Na, K, Rb, Cs) in the absence of iron salt.[32] The anion also has a slight influence on the rate, since the Na and K chlorides (entries 6 and 7) yield slightly lower rates than the corresponding bromides. These trends correspond to those previously observed for the $FeBr_2$/salt-catalysed ATRP.[33]

Table 2. MMA bulk polymerisation in the presence of $FeBr_3$ and bromide or chloride salts.[a]

Entry	Salt	Time /h	Conv /%	$M_{n,GPC}(M_{n,th})$ /Kg mol^{-1}, Đ
1	LiBr	2.5	9.8	2.1(2.0), 1.14
2	NaBr	4.5	60.3	12.8(12.1),1.30
3	KBr	4.5	58.5	12.3(11.7),1.21
4	RbBr	24	-	-
5	CsBr	24	-	-
6	NaCl	5	53.1	11.1(10.6),1.29
7	KCl	8	41.1	9.3(8.2)1.34

[a]Conditions: [MMA]:[$FeBr_3$]:[Salt]:[EBrPA] = 200:0.5:4:1; T = 90°C.

The polymerisations with the Na and K chlorides and bromides were analysed in greater details and the results are shown in Figure 5 (data in Table S9). It is to be noted that all these polymerisations show first order kinetics with a significant positive intercept, suggesting the presence of an initial uncontrolled phase. This obviously reflects onto the polymer dispersities, which are significantly greater than for the polymers produced in the presence of the carbonates and other inorganic additives shown in the previous sections. In all evidence, a temperature of 90°C is too high to insure appropriate control of the $FeBr_2$-catalyzed ATRP of MMA, whereas near-zero intercepts and better control were previously achieved by using $FeBr_2$ (with 10% of $FeBr_3$) in the presence of the same halide salts at 70°C.[33] Another point of interest is that, although the MMA ATRP catalysed by $FeBr_2$/salt are faster with the Na and K halide additives than with the carbonates,[33] the opposite is true for the present polymerisations catalysed by the corresponding $FeBr_3$/salt system. Since the observed rate constant in ATRP depends on the [$FeBr_2$]/[$FeBr_3$] ratio and since, after the initial $FeBr_3$ reduction, the polymerisations proceed through the same moderating equilibrium, these results suggest that the initial $FeBr_3$ reduction proceeds to a lower extent with the halides salts.

(d) Polymer characterisation

An important question concerns the nature of the polymer chain end, because previous studies, as detailed in the introduction, have shown the ability of MMA to reduce $FeBr_3$ and produce methyl 1,2-dibromoisobutyrate.[28, 31] However, contrasting evidence has been presented on the ability of this molecule to act as an ATRP initiator. The use of FeX_3/PPh_3 (X = Cl, Br) as activator, without any external initiator, was shown to produce PPMA-X and the ^{1}H and ^{13}C NMR analyses of the polymer gave some evidence in support of the presence of the $-C(CH_3)(COOCH_3)(CH_2X)$ α-chain end.[28] However, a separate study has shown that the $BrCH_2C(Me)(Br)COOMe/FeBr_2/PPh_3$ system is unable to initiate the MMA polymerisation.[29] In fact, another independent study has shown that PPh_3 is able to abstract Br_2 from $BrCH_2C(Me)(Br)COOMe$, yielding Ph_3PBr_2 and MMA.[34] The action of 1,2-dibromoisobutyrate as a secondary initiator when the MMA polymerisations were carried out in the presence of $FeBr_3$ and another external initiator such as EBriB,[21-24] EBrPA[30] and others[23] has generally not been verified. Only in one case, the ^{1}H NMR analysis of the MMA-Br obtained in the presence of $FeBr_3$ and EBriB gave evidence for the presence of the $-C(CH_3)_2COOEt$ α-chain end[28] but could not exclude or quantify the presence of chains produced by the secondary initiator.

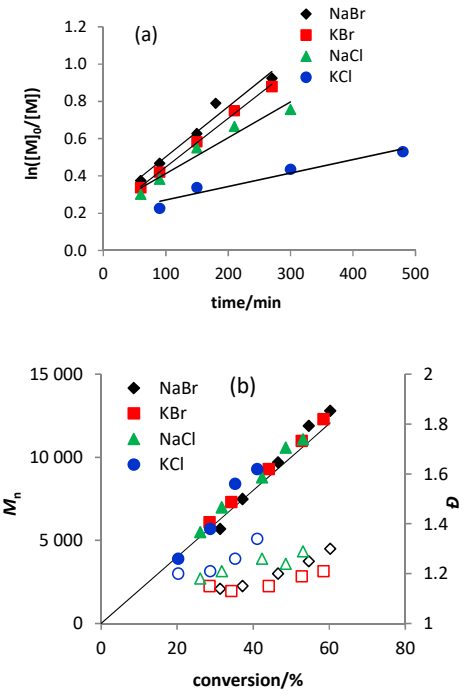

Figure 5. First-order plots (a) and evolution of M_n and $Đ$ with conversion (b) for the EBrPA-initiated bulk MMA polymerisation catalysed by $FeBr_3$ in the presence of different halides salts. [MMA]:[$FeBr_3$]:[Salt]:[EBrPA] = 200:0.5:4:1; T = 90°C.

A short-chain PMMA-Br product (M_n = 2171 g mol^{-1}, $Đ$ = 1.10) obtained by the bulk polymerisation at 60°C in the presence of $FeBr_3/Na_2CO_3$ ([MMA] : [$FeBr_3$] : [Na_2CO_3] : [EBrPA] = 50:0.25:2:1) up to 30% monomer conversion, was analysed by ^{1}H and ^{13}C NMR spectroscopy in greater depth than in any of the

above-mentioned studies. The ^{1}H NMR spectrum in $CDCl_3$ (Figure 6) clearly shows the $–CH_2C(CH_3)(COOCH_3)$-Br ω-chain end as a resonance *a'* at δ 3.73, which is characteristic of the methoxy group, downfield-shifted from the main resonance *a* of the polymer chain at δ 3.57 by the electronic effect of the Br atom. Two closely spaced resonances are in fact visible, as is expected from the two possible terminal *m* and *r* diads. The same resonance for other PMMA-Br chains was reported at δ 3.78 in DMSO-d_6,[19] and at 3.77[35] or 3.80[36] in $CDCl_3$. The presence of the –CH(Ph)COOEt α-chain end from the EBrPA initiator is also clearly visible from the resonances *b* (δ 3.95-4.15; Et CH_2, 2H) and *c* (δ 7.1-7.3; Ph, 5H), matching with those previously reported for other EBrPA-initiated PMMA-Br polymers.[19, 36] Importantly, integration of the α- and ω-chain end resonances yields essentially a 1:1 ratio, indicating that no significant fraction of the recovered macromolecules is initiated by 2,3-dibromoisobutyrate. The presence of the $–C(CH_3)(COOCH_3)(CH_2Br)$ α-chain end cannot be reliably established from the ^{1}H NMR spectrum. In the PMMA-Br made from the initiator-free $FeBr_3$-catalyzed ATRP, the $-CH_2Br$ group was considered responsible for a resonance at δ 3.65.[28] Our PMMA-Br indeed shows a small resonance near that position (see Figure 6) but given its intensity it cannot be assigned to that function and this casts doubts on the previously published assignment.

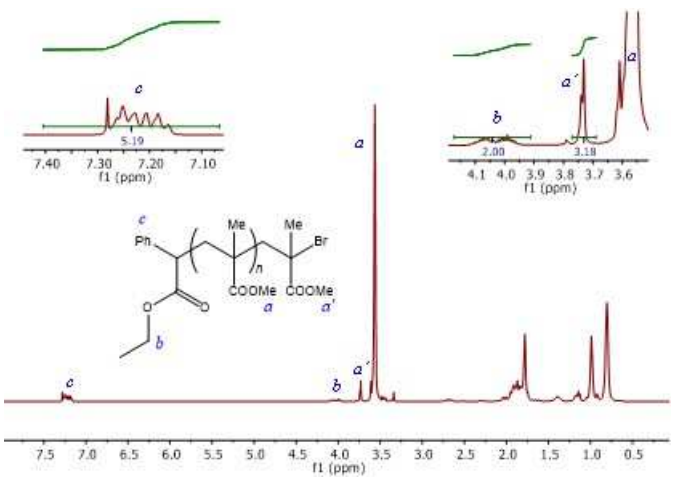

Figure 6. ^{1}H NMR spectrum in $CDCl_3$ of the PMMA-Br (M_n = 2171 g mol^{-1}, $Đ$ = 1.10) produced by bulk polymerisation ([MMA]:[$FeBr_3$]:[Na_2CO_3]:[EBrPA] = 50:0.25:2:1) and stopped at 30% conversion.

The analysis of the ^{13}C spectrum provides additional information. The major resonances are as expected for a PMMA chain, see Figure 7. Particularly, the carbonyl region of the spectrum (δ 171-179) shows the resonances of the in-chain ester functions (*a*) between 176 and 179 ppm, with very similar pattern to that previously reported for atactic PMMA made by the radical route,[28] plus two smaller groups of resonances (*a'* and *a''*) assigned respectively to the ester groups of the α- and ω-chain ends. The group of resonances observed around δ 172 (*a''*) is tentatively assigned to the ω-chain end, because the spectrum of a PMMA-Cl sample was shown to display resonances in the same region.[28] The Ph substitution at the α-chain end causes a different shielding effect, shifting the resonances to the region between 173 and 174 ppm (*a'*). Note that both regions are characterised by more than one resonance because of the various stereochemical possibilities.

The phenyl C atoms give several resonances (*b*), around 140 ppm for *ipso* and in the 124-127 ppm region for *ortho*, *meta* and *para*. Again, these are split by the stereochemical relationship with the first MMA chain unit. Another most characteristic region of the spectrum is between 58 and 61 ppm (see excerpt in Figure 7), where two main groups of resonances are observed around 58.5 and 61 ppm. Assignment of these resonances is aided by the ^{13}C-DEPT135 spectrum, shown in Figure S7 in comparison with the regular ^{13}C{^{1}H} spectrum. The resonances at 61 ppm point downward in the DEPT spectrum, allowing their unambiguous assignment to the ethyl CH_2 group of the α-chain end (*c*), whereas the resonances around 58.5 ppm are absent in the DEPT spectrum and therefore must belong to the quaternary C atom of the ω-chain end (*d*). The corresponding PMMA-Cl spectrum revealed these resonances further downfield (δ around 66 ppm), which is as expected given the higher electronegativity of Cl.[28] Incidentally, the pattern shown by the DEPT spectrum also allows confirmation of the *b* resonance assignments (the *ipso* resonances at ca. 140 ppm are absent in the DEPT135 spectrum) and the identification of the main chain CH_2, CH_3 and C resonances through the main resonances that are respectively pointing down, up or absent. The small resonance at 26 ppm (*e*), downfield from the main chain CH_3 resonances and pointing up in the DEPT spectrum, is assigned to the Me group of the ω-chain end.

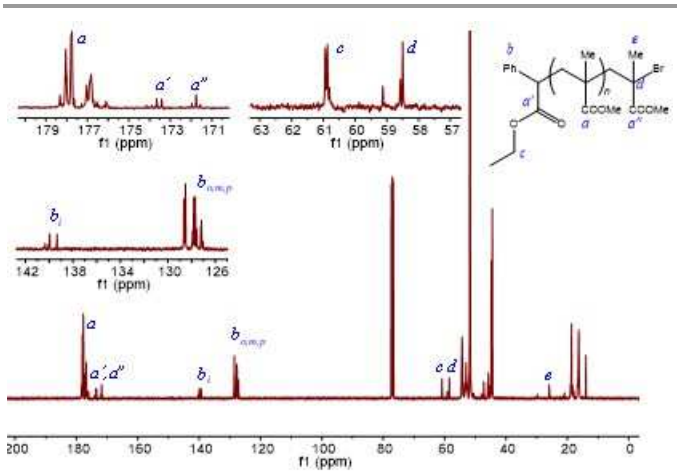

Figure 7. ^{31}C{^{1}H} NMR spectrum in $CDCl_3$ of the PMMA-Br (M_n = 2171 g mol^{-1}, $Đ$ = 1.10) produced by bulk polymerisation ([MMA]:[$FeBr_3$]:[Na_2CO_3]:[EBrPA] = 50:0.25:2:1) and stopped at 30% conversion.

In conclusion, all resonances expected for the EBrPA-initiated macromolecules, $PhCH(COOEt)-(MMA)_n-CH_2CMe(COOMe)$-Br, have been clearly identified. There is no clear evidence, particularly as a result of the ^{1}H NMR signal integration, in favour of the presence of macromolecules with the $–C(CH_3)(COOCH_3)(CH_2Br)$ α-chain end. Further evidence against the presence of such chains comes from the ESI-MS characterisation.

The ESI-MS of a chloroform solution of the recovered polymer is shown in Figure S8. It shows three main distributions, one of which corresponds to the expected PhCH(COOEt)-MMA$_n$-Br+Na$^+$ formulation (distribution with maximum intensity at m/z = 1668 for n = 14), a second one to the same chain with double charge (PhCH(COOEt)-MMA$_n$-Br+2Na$^+$) and the third one to the PhCH(COOEt)-MMA$_n$-C$_8$H$_{11}$O$_4$+Na$^+$ formulation (distribution with maximum intensity at m/z = 1071.5 for n = 7), which is obtained by elimination of CH_3Br and cyclisation between the last two monomer units to generate a lactone at the ω chain end. The latter had previously been reported as the main distribution in the MALDI-TOF spectra of PMMA samples.[37, 38] The distribution with the Br ω chain end was not at all visible when the polymer was analysed by the MALDI-TOF method, consistent with the well-known tendency for Br-terminated polymers to undergo dehydrohalogenation in MALDI-TOF-MS analyses.[38] The ESI-MS also shows a few additional very minor distributions, better visible in the excerpt of Figure S8(b), but none of these seems to correspond to the macromolecules initiated by methyl 1,2-dibromoisobutyrate and terminated by Br.

(e) Mechanistic studies

As mentioned in the introduction, previous contributions have proposed that the monomer itself can reduce $FeBr_3$ to $FeBr_2$, producing methyl 1,2-dibromoisobutyrate, which would supposedly serve as initiator.[28] That system, however, also contains a phosphine ligand, which is also a potential reducing agent for Fe^{III}. A more recent study has shown that, in the absence of phosphine, $FeBr_3$ and MMA can indeed produce $FeBr_2$ and methyl 1,2-dibromoisobutyrate, but the reaction takes place only upon irradiation at room temperature, whereas no conversion was observed after 24 h at 60°C in the absence of light.[30] In addition, it was shown that independently made methyl 1,2-dibromoisobutyrate does not initiate the MMA polymerisation in combination with the $FeBr_2$/PPh_3 activator.[29] These literature precedents raise two questions in relation to our experimental observations: (*i*) how is $FeBr_3$ reduced to produce the $FeBr_2$ activator, and (*ii*) what are the reduction co-products and do they interfere with the polymerisation, notably in the initiation step?

First, we have also independently prepared methyl 1,2-dibromoisobutyrate and tested it as initiator in the presence of either $FeBr_2$/Na_2CO_3, $FeBr_2$/KBr or $FeBr_2$/(nBu$_4$N)Br as activator at 60°C. However, in no case did we observe any polymerisation, even without special protection from normal laboratory light. Thus, it seems that, even if MMA were able to reduce $FeBr_3$ to yield methyl 1,2-dibromoisobutyrate and $FeBr_2$,[28, 31] the combination of these products is nevertheless ineffective to initiate the MMA polymerisation in the presence of the inorganic salts. This result agrees with the polymer characterisation, which clearly shows that most, if not all, macromolecules are initiated by EBrPA (see previous section). Under our operating conditions, like in the previous photochemical study,[30] no potentially reducing phosphine ligand is present, while MMA was demonstrated ineffective as a reducing agent in the absence of additives. Hence, $FeBr_3$ must be converted to the $FeBr_2$ activator by another reduction mechanism, followed by a regular ATRP with $FeBr_2$/EBrPA as activator/initiator pair, as demonstrated in numerous previous contributions.[8-30, 33]

In a recent study,[32] we have shown how inorganic salts (Mt$^+$X$^-$), including alkali metal carbonates and halides, are able to activate EBrPA in the absence of iron complexes to initiate the MMA radical polymerisation, although in an uncontrolled manner. This occurs by atom transfer with formation of the EPA radical and the Mt$^+$(BrX$^\bullet$)$^-$ radical adduct. In a subsequent contribution, however, we have shown that the polymerisation becomes controlled when $FeBr_2$ is added to the system.[33] In order to learn more about the $FeBr_3$ reduction, we have run a few stoichiometric experiments with GC-MS analysis. All these experiments involved heating $FeBr_3$ at 90°C in MeCN for 2 h in the presence of different additives, the resulting solutions were analysed by GC-MS and the product identity, which was suggested by the MS (spectra collected in the SI section), was confirmed by the corresponding analysis of genuine samples, when available. The GC traces of the most relevant studies are collected in Figure 8, while the identity of the main products and their formation mechanism are proposed in Scheme 2.

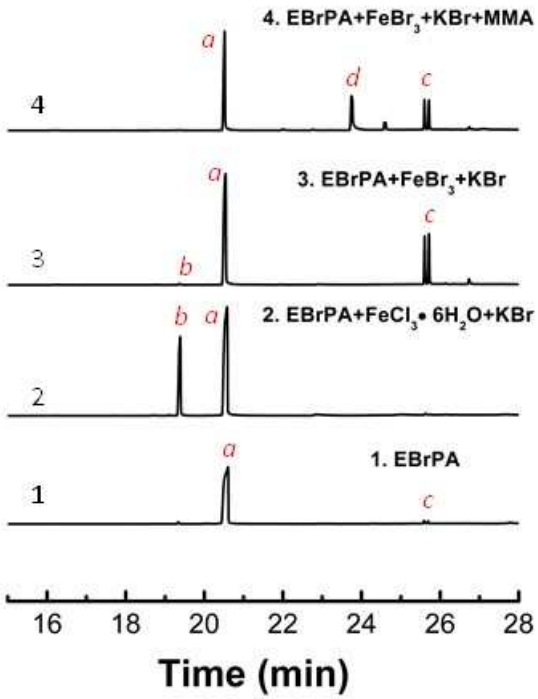

Figure 8. Gas-chromatograms of EBrPA (0.0472 M in MeCN) after heating at 90°C for 2 h in the presence of different additives at the concentration of 0.0472 M for the Fe complexes and 0.0944 M for KBr or KOH.

The GC trace of Figure 8.1 was obtained for the starting EBrPA solution before heating. It shows, in addition to the main peak of EBrPA at 20.70 min (labelled *a*, MS in Figure S11), two small peaks labelled *c* at 25.66 and 25.78 min. After heating for 2 h in MeCN, the resulting GC trace does not significantly change. Figure 8.2 shows the GC trace obtained after heating EBrPA in the presence of $FeCl_3$·$6H_2O$/KBr. There are two main peaks of

nearly equivalent intensity, one for the unreacted EBrPA and the other one at 19.48 min (labelled *b*, MS in Figure S12) for the halide exchange product, EClPA. This result is consistent with the previously described[32] atom transfer activation of EBrPA by KBr, yielding $PhCH^{\bullet}(COOEt)$ and $K(Br_2^{\bullet})$, followed by deactivation of the EPA radical by $FeCl_3$ and final reoxidation of $FeCl_2$ by $K(Br_2^{\bullet})$ (Scheme 2). Replacing KBr with KOH gave a substantially identical result (see Figure S13). When the same experiment was carried out in the presence of $FeBr_3$/KBr, peak *b* was still observed but only with a very small intensity (the formation of EClPA probably results from the presence of a minor Cl impurity in the commercial $FeBr_3$), whereas the two peaks *c* were now present with much greater intensity than in the starting material (Figure 8.3). The MS characterisation (Figure S14 suggests that these peaks belong to the two diastereomeric products (*meso* and *dl*) of EPA radical coupling, diethyl 2,3-diphenylsuccinate. Hence, these two compounds are already present as contaminants in commercial EBrPA, but their formation is promoted by the Br atom transfer activation in the absence of monomer. The fact that these products do not form in significant quantities in the presence of $FeCl_3$ can be rationalised by the fact that the deactivation of the EPA radical by Cl atom transfer from $FeCl_3$, yielding EClPA (*c*), is not only faster than dimerisation, but also irreversible. In the presence of $FeBr_3$, on the other hand, the corresponding deactivation by $FeBr_3$ (also shown in Scheme 2) yields back EBrPA, which can be continuously reactivated and eventually the EPA radical can terminate by coupling and accumulate. It is important to underline that this dimerisation will be less prevalent under polymerisation conditions, where the high monomer concentration favours addition to monomer. An essentially identical result was obtained when the EBrPA/$FeBr_3$ system was activated by KOH instead of KBr (see Figure S15). Note, however, that this GC trace also shows several additional small peaks, two of which (at 16.00 and 26.11 min), will be further discussed below.

From the stoichiometric point of view, the EPA radical coupling cannot account for the reduction of $FeBr_3$. Rather, it entails the accumulation of an equivalent amount of $K(BrX^{\bullet})$ radicals, which contribute to reoxidise $FeBr_2$ to $FeBr_3$. Only the EPA radical deactivation by $FeBr_3$ produces $FeBr_2$ (and deactivation by $FeCl_3$ produces $FeCl_2$). In terms of the desired accumulation of the Fe^{II} activator, an excess of organic radicals (reducing equivalents) is beneficial, whereas an excess of $K(BrX^{\bullet})$ radicals (oxidizing equivalents) is detrimental. Thus, the disappearance of the EPA radicals by dimerisation is detrimental. The only possible conditions leading to the accumulation of Fe^{II} is a dominant disappearance of the $K(BrX^{\bullet})$ radicals. The experiments of Figure 8.2 and Figure 8.3 reproduce the polymerisation conditions, except for the presence of the MMA monomer. Therefore, during polymerisation, the Fe^{II} activator could result from the removal of the oxidizing $K(BrX^{\bullet})$ radicals by MMA, supposedly yielding methyl 1,2-dibromoisobutyrate. It is relevant to underline that the primary product of the $K(BrX^{\bullet})$ addition to MMA, namely the $BrCH_2C^{\bullet}(CH_3)(COOCH_3)$ radical, could add to MMA and generate additional growing chains. This is, however, excluded by the absence of such chains according to the NMR and ESI-MS characterisation. We propose that the absence of such reactivity results from the additional stabilisation of the primary radical by the effect of the γ-Br atom, as shown in Scheme 3. Therefore, only further quenching by a second $K(BrX^{\bullet})$ transient may occur to yield methyl 1,2-dibromo-isobutyrate.

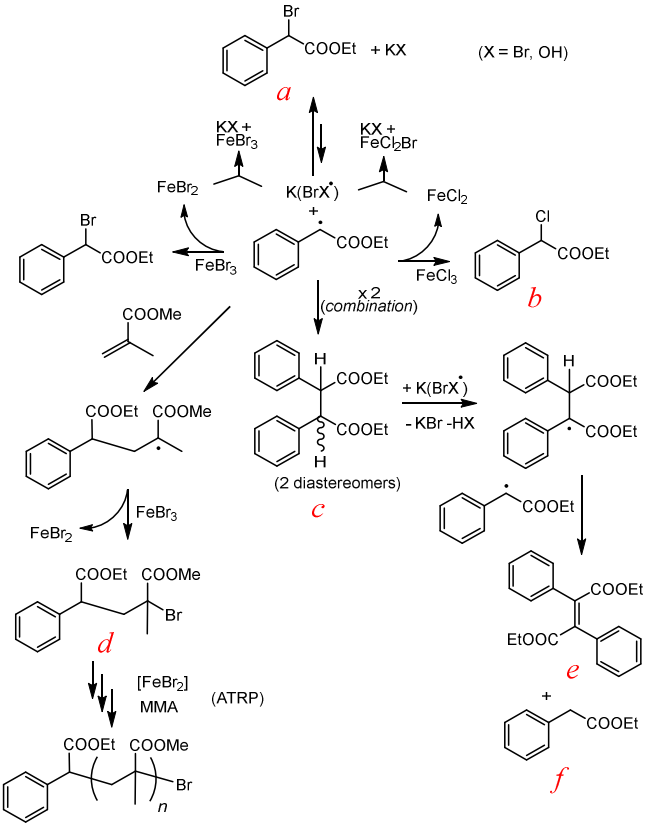

Scheme 2. KX-activated (X = Br or OH) Br atom transfer for the EBrPA ATRP initiator and subsequent evolution of the EPA radical.

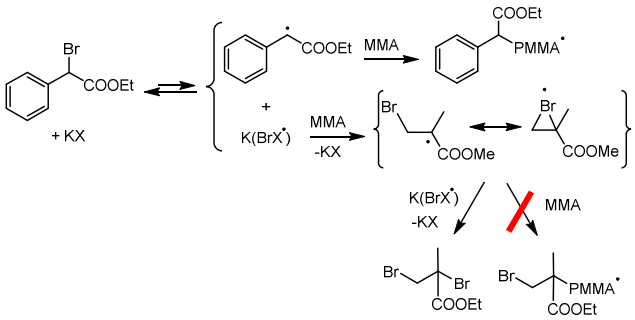

Scheme 3. Possible reason for the absence of $BrCH_2C^{\bullet}(CH_3)(COOCH_3)$ α-chain ends in MMA polymerisation.

Additional experiments were carried out in the presence of MMA in order to confirm the formation of methyl 1,2-dibromoisobutyrate. In a first experiment, $FeBr_3$ and KBr were heated in MeCN in the presence of MMA and without the EBrPA initiator. The GC of the resulting solution does not show the formation of any product: neither MMA nor methyl 1,2-dibromoisobutyrate could be detected. A control experiment revealed that a solution of MMA in MeCN does not produce any

observable peak, probably because MMA is polymerised inside the column of our GC instrument. On the other hand, methyl 1,2-dibromoisobutyrate is eluted from the column with a retention time of 11.26 min (Figure S16). The lack of thermal reduction of $FeBr_3$ by MMA is consistent with a recent report,[31] which demonstrated that this reaction takes place only under UV light irradiation. This result is also consistent with the absence of thermal polymerisation for the initiator-free $FeBr_3$/MMA combination.[29]

A new experiment was then carried out for a solution containing EBrPA, $FeBr_3$, KBr, and MMA (1 equivalent). Running the experiment with greater amounts of MMA (i.e. under conditions closer to those of the polymerisation) would not be informative because it would lead to MMA polymerisation. In the GC trace of the resulting solution, shown in Figure 8.4, a peak corresponding to methyl 1,2-dibromoisobutyrate is not visible, but a new product, which is characterised by a peak at 23.74 min (labelled *d*), is observed. The MS of this compound (shown in Figure S17) did not find a match in the library of our GC-MS instrument. A reasonable mechanistic proposition is that the generated EPA radical adds to MMA, as in the polymerisation initiation phase, yielding the $PhCH(COOEt)CH_2$-$C^{\bullet}(CH_3)(COOMe)$ radical, which is then quenched, possibly by the $K(Br_2^{\bullet})$ radical to yield the ATRP unimer (see Scheme 2). The heaviest fragment in the spectrum (m/z = 234) matches with the formulation $[PhCH(COOEt)CH_2C(CH_3)(COOMe) - C_2H_4]^+$ and suggests the possible ionisation by Br^- loss and ethylene elimination from the ethyl ester group. Therefore, we make the tentative but reasonable proposition that the ATRP unimer is the product corresponding to the observed peak *d*. When the same experiment was repeated using KOH in place of KBr, a very similar product distribution was observed, but the peak of product *d* at 23.74 min is much more prominent, see Figure S18(a). This agrees with the greater efficiency of KOH as activator for EBrPA relative to KBr.[32] In addition, the same two peaks already observed in the EBrPA/$FeBr_3$/KOH experiment (Figure S15) at 16.00 and 26.11 min are also observed here. Finally, this GC trace also reveals a very small peak at 11.26 min, the identity of which as methyl 1,2-dibromoisobutyrate was confirmed by the MS, see Figure S18(b). Thus, the hypothesis that the oxidizing $K(BrX^{\bullet})$ equivalents are removed by MMA is confirmed.

Two final experiments were run to verify the fate of the radicals produced by the EBrPA activation, using either KBr or KOH as activators without any other additive ($FeBr_3$ or MMA). The results are shown in Figure 9. The GC trace of the solution obtained using KBr, shown in Figure 9.1, shows quite unexpectedly a very low conversion of EBrPA. Only very small amounts of EClPA (*b*) and the EPA radical dimerisation products *c* are visible. In comparison with the GC trace of Figure 8.3, obtained under the same conditions of solvent, temperature, time and concentrations but in the presence of $FeBr_3$ (1 equivalent), the slower conversion reveals that $FeBr_3$ must act as a catalyst for the EBrPA activation by KBr. This may involve, for instance, the homolytic labilisation of the C-Br bond by interaction of a Br lone pair with the Lewis acidic Fe^{III} center. Alternatively, the interaction between KBr and $FeBr_3$, yielding $K[FeBr_4]$ may enhance the Lewis acidity of K^+, resulting in the same homolytic C-Br bond labilisation.[39] The second experiment, using KOH, leads to the GC trace shown in Figure 9.2. In this case, the activation is very efficient, leaving no residual EBrPA after the 2 h heating period. The faster activation of EBrPA by KOH than by KBr is, once again, as expected.[32] A second relevant observation is that products *c* are again formed in large amounts, but in this case the process also leads to the formation of two additional major products, *e* and *f*, at 16.00 and 26.11 min. These are the same peaks observed in the experiments of Figure S15 and Figure S18(a). These products were identified by MS as diethyl 2,3-diphenylfumarate and ethyl phenylacetate, respectively (see Figure S19). Their formation can be easily rationalised as shown in Scheme 2. In the absence of rapid quenching of the hydroxyl radical by MMA (or by disproportionation, *vide infra*), the latter can react with the most activated C-H bond, namely one of the benzylic C-H bonds of *c*, to yield a stabilised 2-succinyl radical. The latter can then transfer one of the H atoms at the 3 position to a primary EPA radical, yielding the two observed products simultaneously. Other products that are generated in small amounts, see Figure 9.2, most likely resulting from other secondary radical reactions, could not be unambiguously identified by MS.

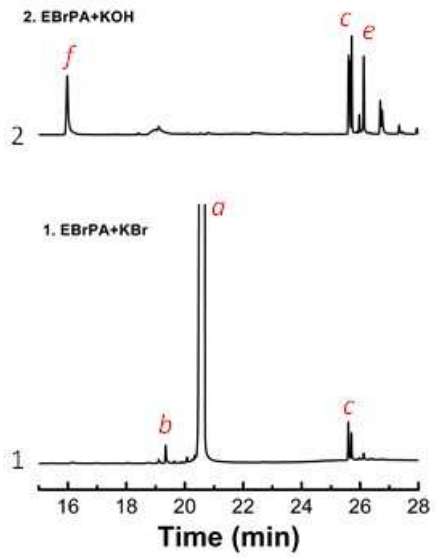

Figure 9. Gas-chromatograms of EBrPA (0.0472 M in MeCN) after heating at 90°C for 2 h in the presence of KBr or KOH (0.0944 M).

There is one important difference between the two $Mt^+(BrX^{\bullet})^-$ radicals (X = Br, OH). Whereas $K(Br_2^{\bullet})$ can only be quenched by a reductant, $K(BrOH^{\bullet})$ may also disproportionate via dimerisation to H_2O_2 to eventually afford H_2O and O_2. According to the literature, this reaction is efficiently catalysed by iron salts (*catalase* activity).[40-42] Thus, when the activation of EBrPA is carried out in the presence of $FeBr_3$ (or $FeCl_3$), the $K(Br_2^{\bullet})$ oxidizing equivalents produced by the KBr activation may only be removed by $FeBr_2$ and MMA, whereas $K(BrOH^{\bullet})$ may also disappear by Fe-catalysed disproportionation without consuming reducing equivalents, hence allowing a greater accumulation of the Fe^{II} ATRP activator and a faster

polymerisation. This agrees with the experimentally observed polymerisation rates: the k_{obs} for the $FeBr_3$/KOH (Table S8) and $FeBr_3/K_2CO_3$ (Table S1) systems at 60°C is similar and much higher than for the $FeBr_3$/KBr system, for which reasonable rates could only be achieved at 90°C (Table S9). In retrospect, the absence (or presence in very small amounts) of products *e* and *f* in all the experiments run in the presence of $FeCl_3$ or $FeBr_3$, and particularly those using the faster activator KOH (Figure S13 and Figure S15) must result from a more efficient disappearance of the K($BrX^{\bullet}$), which, for the KOH case, may also have an important contribution from the Fe^{III}-catalysed disproportionation.

In conclusion, the removal of the oxidizing K($BrX^{\bullet}$) equivalents (by addition to MMA or disproportionation) prevails, leading to the Fe^{II} ATRP activator accumulation, whereas disappearance of the reducing $EPA^{\bullet}$ equivalents by coupling (as well as the bimolecular terminations of the growing polymer chains) is suppressed by the persistent radical effect. Obviously, the time required for the processes illustrated in Scheme 2 to take place rationalizes quite well the induction time observed for most MMA polymerisations promoted by the $FeBr_3$/EBrPA/salt systems.

Conclusions

The present study has illustrated how it is possible to implement the ATRP of MMA, with excellent control, under operationally simpler and more economic conditions than ever before. The process is solvent-free and uses air stable, inexpensive and easily available $FeBr_3$ and alkali metal additives, in combination with EBrPA as initiator. Thus, it represents an improvement with respect to the related process that uses $FeBr_2$ under otherwise identical conditions[33] and also with respect of all other previously reported iron-based ATRP protocols, realizing truly "ligand-free" conditions. This allows easier purification for mass production, making ATRP environmental friendlier and thus more attractive. The $FeBr_2$ ATRP activator is made *in situ* by $FeBr_3$ reduction. This process does not occur by the direct action of the monomer under thermal conditions. Rather, it starts with the EBrPA activation by the inorganic additive, Mt^+X^-, to yield $EPA^{\bullet}$ and $Mt^+(BrX^{\bullet})^-$.[32] The oxidizing $Mt^+(BrX^{\bullet})^-$ is then removed by MMA, or by Fe^{III}-catalysed disproportionation (for X = OH), making it possible for $EPA^{\bullet}$ to reduce $FeBr_3$ by atom transfer. Subsequently, regular ATRP can proceed as in the previously reported EBrPA-initiated MMA polymerization catalysed by $FeBr_2$ in the presence of inorganic salts.[33] Thus, the process has elements in common with AGET (Activator Generated by Electron Transfer) ATRP,[43, 44] but differs from it because the reducing agent (namely, the EPA radical) is not directly added to the system but is rather generated by pathways that remove oxidizing equivalents (namely the bromine radical of EBrPA).

Conflicts of interest

There are no conflicts to declare.

Acknowledgements

This work was financially supported by the National Natural Science Foundation of China (51622303) and Natural Science Foundation of Hubei Scientific Committee (2018CFA059 and 2016CFA001). We also gratefully acknowledge the CNRS (Centre National de la Recherche Scientifique) for recurrent funding and the China Scholarship Council for a doctoral fellowship to JW (No. 201806160052).

Notes and references

1. K. Matyjaszewski and N. V. Tsarevsky, *J. Am. Chem. Soc.*, 2014, **136**, 6513-6533.
2. M. Ouchi and M. Sawamoto, *Macromolecules*, 2017, **50**, 2603-2614.
3. X. C. Pan, M. Fantin, F. Yuan and K. Matyjaszewski, *Chem. Soc. Rev.*, 2018, **47**, 5457-5490.
4. K. Matyjaszewski, *Advanced Materials*, 2018, **30**, 1706441.
5. T. G. Ribelli, F. Lorandi, M. Fantin and K. Matyjaszewski, *Macromol. Rapid Comm.*, 2019, **40**, 1800616.
6. R. Poli, L. E. N. Allan and M. P. Shaver, *Prog. Polym. Sci.*, 2014, **39**, 1827–1845.
7. Z. Xue, D. He and X. Xie, *Polym. Chem.*, 2015, **6**, 1660-1687.
8. Z. Xue, S. K. Noh and W. S. Lyoo, *J. Polym. Sci., Part A: Polym. Chem.*, 2008, **46**, 2922-2935.
9. X. P. Chen and K. Y. Qiu, *Macromolecules*, 1999, **32**, 8711-8715.
10. D. Q. Qin, S. H. Qin, X. P. Chen and K. Y. Qiu, *Polymer*, 2000, **41**, 7347-7353.
11. X. P. Chen and K. Y. Qiu, *Chem. Comm.*, 2000, 233-234.
12. X. P. Chen and K. Y. Qiu, *New J. Chem.*, 2000, **24**, 865-869.
13. K.-Y. Qiu, P. Li and X.-P. Chen, *Macromol. Symp.*, 2003, **195**, 33-38.
14. S.-H. Qin, D.-Q. Qin and K.-Y. Qiu, *New J. Chem.*, 2001, **25**, 893-895.
15. C. Jian, J. Chen and K. D. Zhang, *J. Polym. Sci., Polym. Chem.*, 2005, **43**, 2625-2631.
16. G.-X. Wang, M. Lu, L.-C. Liu, H. Wu and M. Zhong, *J. Appl. Polym. Sci.*, 2013, **128**, 3077-3083.
17. G. Zhu, L. Zhang, Z. Zhang, J. Zhu, Y. Tu, Z. Cheng and X. Zhu, *Macromolecules*, 2011, **44**, 3233-3239.
18. G. X. Wang, M. Lu and Y. B. Liu, *J. Appl. Polym. Sci.*, 2012, **126**, 381-386.
19. J. Wu, X. W. Jiang, L. F. Zhang, Z. P. Cheng and X. L. Zhu, *Polymers*, 2016, **8**.
20. X. P. Chen and K. Y. Qiu, *Chem. Commun.*, 2000, 1403-1404.
21. Z. Xue, T. B. L. Nguyen, S. K. Noh and W. S. Lyoo, *Angew. Chem. Int. Ed.*, 2008, **47**, 6426-6429.
22. Z. Xue, H. S. Oh, S. K. Noh and W. S. Lyoo, *Macromol. Rapid Commun.*, 2008, **29**, 1887-1894.
23. Z. Xue, D. He, S. K. Noh and W. S. Lyoo, *Macromolecules*, 2009, **42**, 2949-2957.
24. X. X. Chen, M. Y. Khan and S. K. Noh, *Polym. Chem.*, 2012, **3**, 1971-1974.
25. Y. Wang, Y. Kwak and K. Matyjaszewski, *Macromolecules*, 2012, **45**, 5911-5915.
26. H. Schroeder, K. Matyjaszewski and M. Buback, *Macromolecules*, 2015, **48**, 4431-4437.
27. H. Aoshima, K. Satoh, T. Umemura and M. Kamigaito, *Polym. Chem.*, 2013, **4**, 3554-3562.

28. M. Y. Khan, X. Chen, S. W. Lee and S. K. Noh, *Macromol. Rapid Commun.*, 2013, **34**, 1225-1230.
29. D. F. Yang, J. R. Wang, J. Y. Han, M. Y. Khan, X. L. Xie and Z. G. Xue, *J. Polym. Sci., Polym. Chem.*, 2017, **55**, 3842-3850.
30. X. Pan, N. Malhotra, J. Zhang and K. Matyjaszewski, *Macromolecules*, 2015, **48**, 6948-6954.
31. X. C. Pan, N. Malhotra, S. Dadashi-Silab and K. Matyjaszewski, *Macromol. Rapid Comm.*, 2017, **38**.
32. J. Wang, J. Han, H. Peng, X. Tang, J. Zhu, R.-Z. Liao, X. Xie, Z. Xue, C. Fliedel and R. Poli, *Polym. Chem.*, 2019, **10**, 2376-2386.
33. J. Wang, J. Han, X. Xie, Z. Xue, C. Fliedel and R. Poli, *Macromolecules*, 2019, **52**, 5366−5376.
34. R. D. Khachikyan, N. V. Tovmasyan and M. G. Indzhikyan, *Russian Journal of General Chemistry*, 2007, **77**, 1034-1036.
35. J. Zhou, J. R. Wang, J. Y. Han, D. He, D. F. Yang, Z. G. Xue, Y. G. Liao and X. L. Xie, *Rsc Advances*, 2015, **5**, 43724-43732.
36. X. R. Shen, D. Z. Xia, Y. X. Xiang and J. G. Gao, *E-Polymers*, 2019, **19**, 323-329.
37. C. D. Borman, A. T. Jackson, A. Bunn, A. L. Cutter and D. J. Irvine, *Polymer*, 2000, **41**, 6015-6020.
38. N. K. Singha, S. Rimmer and B. Klumperman, *Eur. Polym. J.*, 2004, **40**, 159-163.
39. B. Ray, Y. Isobe, S. Habaue, M. Kamigaito and Y. Okamoto, *Polym. J.*, 2004, **36**, 728-736.
40. I. A. Salem, M. El-Maazawi and A. B. Zaki, *International Journal of Chemical Kinetics*, 2000, **32**, 643-666.
41. H. B. Dunford, *Coord. Chem. Rev.*, 2002, **233**, 311-318.
42. A. Ghosh, D. A. Mitchell, A. Chanda, A. D. Ryabov, D. L. Popescu, E. C. Upham, G. J. Collins and T. J. Collins, *J. Am. Chem. Soc.*, 2008, **130**, 15116-15126.
43. W. Jakubowski and K. Matyjaszewski, *Macromolecules*, 2005, **38**, 4139-4146.
44. K. Min, H. Gao and K. Matyjaszewski, *J. Am. Chem. Soc.*, 2005, **127**, 3825-3830.